Additive Manufacturing of 1018 Steel: Process Observations and Calculations

C. M. Knapp [* †], T. J. Lienert[†], C. Chen[†], and D. Kovar[*],
Solid Free-Form Fabrication Conference: Austin, Texas: August 4-6th 2014

[*] Department of Mechanical Engineering, The University of Texas at Austin: Austin, TX 78731
[†] Material Science and Technology, Los Alamos National Laboratory: Los Alamos, NM 87545

ABSTRACT

The temperature distribution in the vicinity of the laser used in direct metal deposition (DMD) plays a critical role in determining the final microstructure and mechanical properties of the deposit and the heat-affected zone (HAZ) within the substrate. Samples were prepared using Laser Engineered Net Shaping (LENS[TM]) by depositing AISI 1018 steel powder onto AISI 1018 steel substrates in multiple, overwritten passes. The laser power and speed were varied to control the heat input and the rate of cooling. The process characteristics were then quantified and compared across the samples to determine the effect of input parameters on the resulting deposit microstructures.

INTRODUCTION

Additive manufacturing has become mainstream in near-net shape fabrication and manufacturing. More recent efforts have been made to enable direct writing of metallic components that can be used in load-bearing components [1]. To realize this objective it is necessary to understand the relationship between the processing parameters, the morphology of the deposit, and micro- and macro-scale defects that can arise from process instabilities.

Unlike polymer additive manufacturing routes, where extrusion technologies can be used, direct metal deposition requires melting of powders. There are two common methods to generate the necessary energy densities to melt powders in high fusion temperature metals. One option is to use an electron beam, which requires that the entire sample be placed under vacuum. However, a more common approach is to use a continuous-wave laser, such as that used in Laser Engineered Net Shaping (LENS™), which is the subject of this research. This research studies the influence of process input parameters, including laser power, laser speed and powder feed rates, on process efficiencies and the morphology of the deposit. We fabricate a sample that consists of fifty overwritten, one-dimensional deposition passes, to produce a 1.5 dimensional "wall" with an intended final height of 2.54 cm. Following deposition, the samples were examined for defects and the morphology of the deposit was correlated to processing parameters.

EXPERIMENTAL PROCEDURE

DEPOSITION SYSTEM

A LENS[TM] MR-7 (Optomec Inc., Albuquerque, NM) was used to produce the samples used in this study. A schematic of this system is shown below. The system consists of a

continuous wave (CW) 1 kW Yb-fiber laser (1070 nm), an aerosol powder feeder, and a deposition head. The location of the deposition head is controlled using three-axis, computer-numerical control.

The powder feeding system in the LENS^{TM} MR-7 operates by the rotation of a screw type mechanism, which builds up mounds of powder as it rotates. Argon gas is flowed over the top of the mounds of powder that are built up and caries the powder particles towards the deposition head. The powder is fed through four nozzles symmetrically positioned on the deposition head into the focus of the laser beam. As the deposition head moves, molten material is deposited onto the substrate and subsequently cools (shown in orange in Fig. 1).
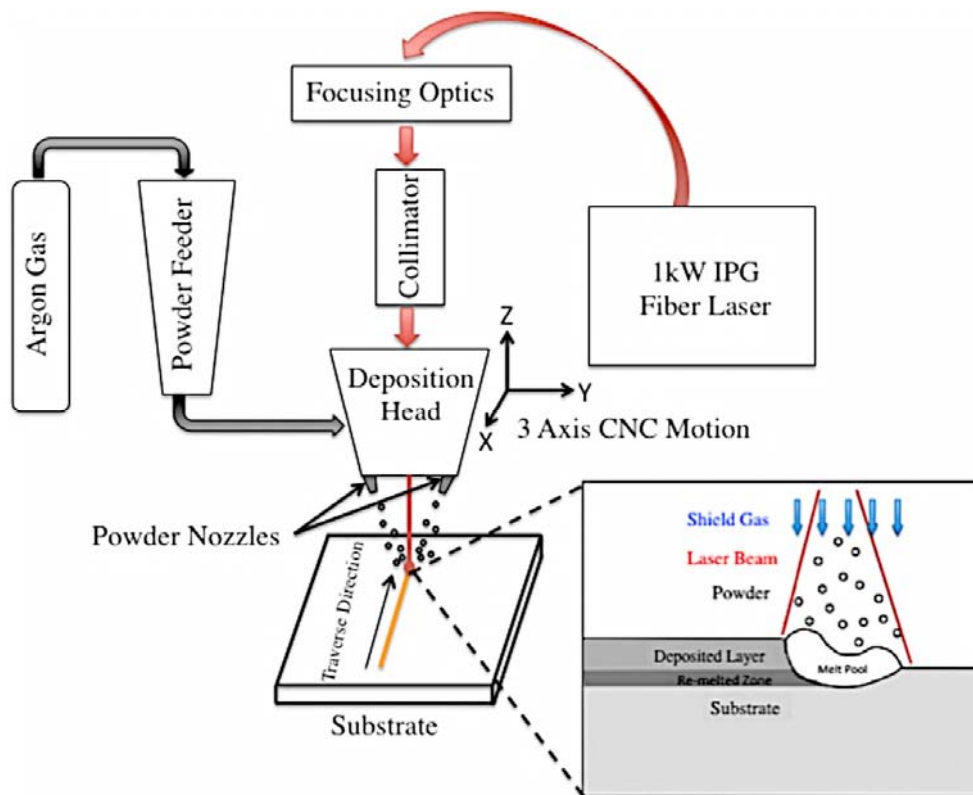

FIGURE 1:SCHEMATIC OF THE LENS^{TM} MR-7 SYSTEM (DEPOSITED MATERIAL SHOWN IN ORANGE) ADAPTED FROM LIOU ET AL. [2]

MATERIAL SYSTEM

AISI 1018 steel was chosen as the material system to be studied because of its wide availability in plate and powder form, and it affords a relatively straightforward temperature-dependent microstructure from which *post-mortem* analysis of the thermal characterization can be inferred.

POWDER

Optomec recommends -80 +325 mesh spherical powder for use in their powder feeders [3]. This size distribution allows for uniform powder supply to the deposition head. Powder size

was determined by mounting powder in epoxy, lightly polishing, and etching to visualize the shape and morphology. The spherical shape and fine grain size shown in Fig. 2 are consistent with the gas atomization process by which the powder was produced by Nuclear Metals Incorporated (Concord, MA, USA).
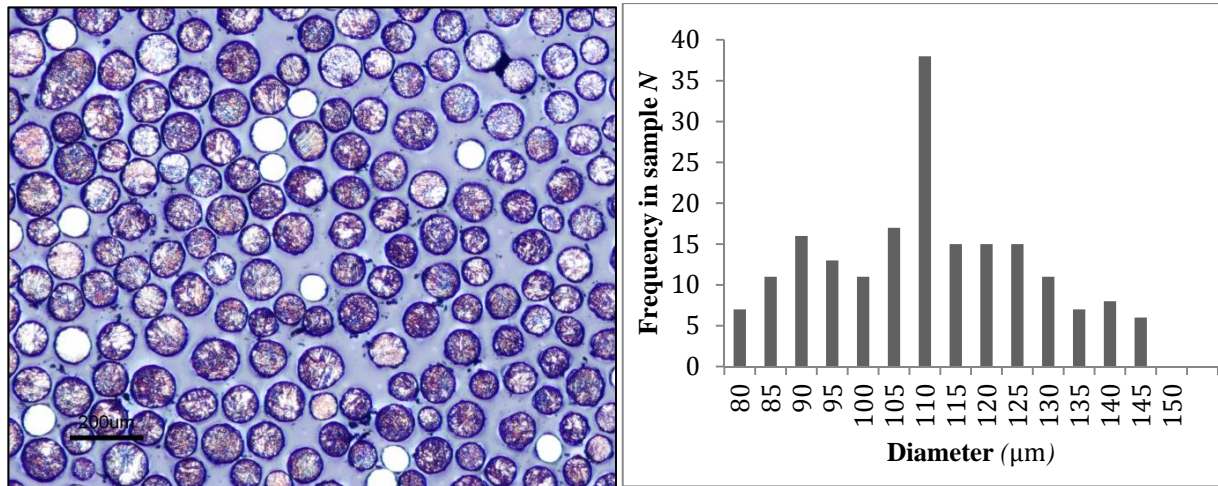

FIGURE 2: (LEFT) EXAMPLE 10× MICROGRAPH OF MOUNTED, UNPROCESSED 1018 POWDER. (RIGHT) POWDER SIZE DISTRIBUTION HISTOGRAM

A series of micrographs similar to the one shown in Figure 2 were compiled and analyzed using ImageJ (1.47v, NIH, Bethesda, MD, USA) image analysis software. A bias is introduced by the optical measurement of particle size distribution from a random cross section. This bias was corrected using the approach presented in Heilbronner *et al.* [4], to obtain the true powder statistics. The true powder diameter mean μ_t is 121 μm and the true standard deviation σ_t is 17.3 μm. While this is 20% larger than the ideal diameter recommended by Optomec Inc. of ~100μm, it is well within the operation window when the powder is spherical in nature and flows well.

SUBSTRATE

AISI 1018 6.35 mm (¼ inch) thick, cold finished, steel substrates were fabricated and marked for three depositions per substrate. The substrates were then bead blasted to decrease reflectivity, and enhance the process efficiency. Four thermocouples each were then spot welded onto the substrate at varying distances from the deposits so that *in situ* thermal measurements could be taken. However the temperature data taken from the thermocouples is outside the scope of this research paper, which focuses on process analysis.

PROCESS PARAMETERS

In order to accurately characterize the process, the initial conditions of the depositions, such as laser power and powder feed rate must be experimentally determined. The powder feed rate is set and controlled by a tachometer that measures the rotational speed of the motor used to feed powder. In order to determine the relationship between rotational speed and powder feed rate, three tests were performed by flowing powder into plastic bags for one minute and then weighing the collected material to determine the amount of powder that had been fed in the allotted time. The three mass flow measurements at varying powder feed revolutions per minute

yielded a relationship between powder feeder speed and mass flow rate. These points were then used to create a regression analysis to obtain mass flow rate of powder as a function of powder feeder revolutions per minute.

To quantify the losses in the system up to the point of the impact of the laser on the substrate, the true laser power was measured using a lollipop-type calorimeter that was placed in the laser focus for a period of 30 seconds. These measurements were done in successive trials to obtain a curve of the actual power produced as a function of laser power demand. The curve was then fit using linear regression so that the actual power could be determined from the power demand. Three trials were conducted with the processing conditions shown in Table 1. The three trials were conducted under conditions of 1) high powder feed rate, and moderate laser power and laser speed, 2) low powder feed rate, laser power, and laser speed, and 3) high powder feed rate, laser power, and laser speed.   A schematic illustration of the sample geometry is shown in Figure 3; a total of fifty successive deposits were overlaid to create a wall that was nominally 2.54 cm (1 inch) tall and 7.62 cm long.

TABLE 1: INITIAL CONITIONS

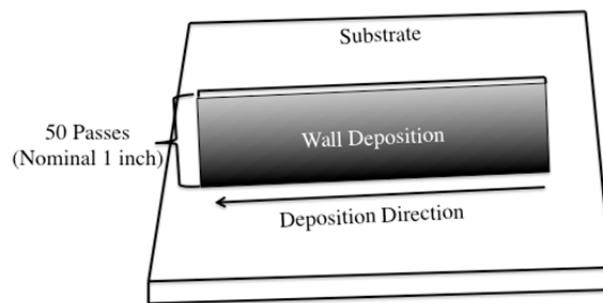| Test #	Initial Powder Feed Rate [g/min]	Laser Power [Watts]	Laser Speed [mm/s]
1	14	430	6.35
2	3.8	290	2.11
3	15	600	19.0

FIGURE 3: 50 PASS WALL DEPOSITION SCHEMATIC

Prior to deposition, the part trajectories must be programmed and the specific powder gas flow levels and motor RPM must be set. The user must then wait for the flow to stabilize before the deposition can be executed. Deposition begins by turning the laser, and loitering at the initial point for fractions of a second prior to the movement of the deposition head. The loitering of the laser is a key difference between selective laser sintering (SLS) and LENS™. In LENS™ full melting is induced and the powder is deposited into the melt pool [5]. Once the melt pool is initiated the deposition head begins to move and the part is slowly built up, pass-by-pass. The optical setup used to produce the deposits maintained the focus of the laser ~300μm beneath the surface of the layer to be deposited. After the completing the first pass, the laser was brought

337

back to the initial position. The successive pass was made in the same way except that the height of the focus was increased by 0.508 mm. The resultant component is shown in Figure 4.
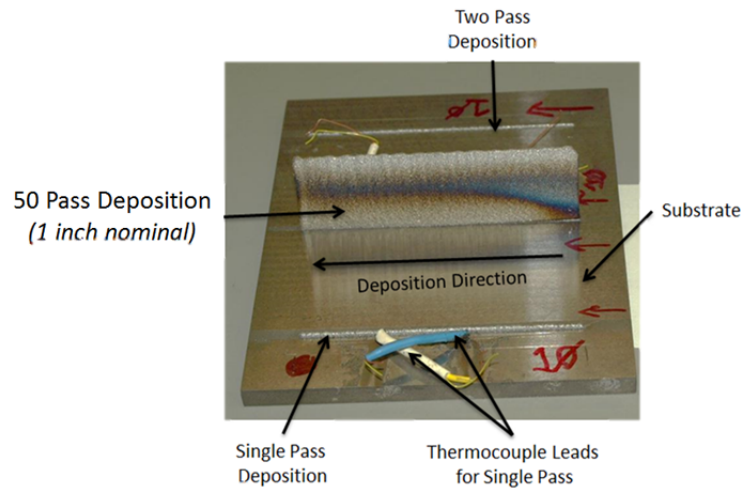

FIGURE 4: COMPLETED DEPOSITIONS (NOTE ASYMMETRIC OXIDE FORMATION)

ANALYSIS OF DEPOSITS

After deposition, the samples were coarsely cut from the plate using an abrasive cut-off saw. Regions of interest were further sectioned to smaller sizes using a low speed saw to minimize the damage to the specimen. After cutting and mounting in Buehler Kwick Kit long cure epoxy (Buehler, Lake Bluff, Illinois, USA), the specimens were ground and polished. The samples were ground using SiC paper and then polished using diamond suspensions on an automatic polisher (Struers Rotopol 11 and RotoForce 1, Westlake, Ohio, USA). A sequence of suspensions starting with 9µm, 3µm, and 1µm was used. The force applied during polishing was 40 N and each of the polishing steps was conducted for 4 minutes. After polishing with the diamond suspensions, a final polishing was conducted with 0.05µm alumina suspension at a force of 30 N for 3 minutes. The samples were then etched using 5% nitric acid and 95% ethanol (5% Nital) to reveal the microstructure. Stereo microscopic images of section of the samples are shown in Fig. 5.
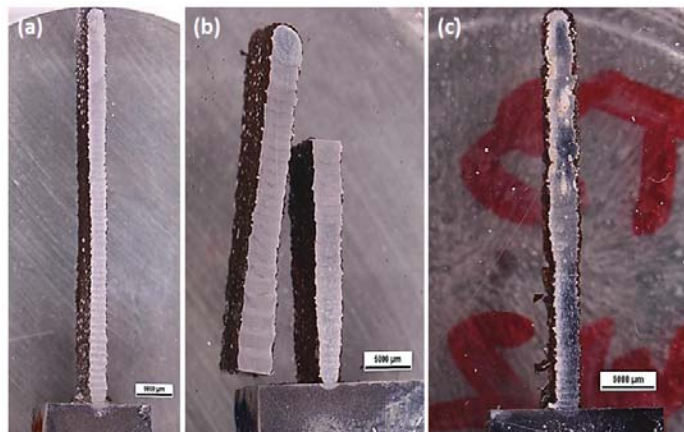
Note that sample 2 (Fig. 5b) was significantly taller than the other two samples; this sample was cut at roughly the mid-plane and the top half of the sample was placed next to the bottom half in order to fit the sample in the mount used for polishing

PROCESS MEASUREMENTS

In order to compare input parameters across tests, specific energy was used and defined to be the supplied laser power divided by the traverse speed. High specific energy occurs at high power and low speed, and the low specific energy occurs at low power and high speed. The specific energy was plotted with the powder feed rates that were supplied to the deposition to show the relationships between laser power, speed, and powder feed rate (Fig 6). However, observation of the deposits revealed that certain powder feed rates were not conducive to stable deposition (shown in red) while others were stable (show in green).
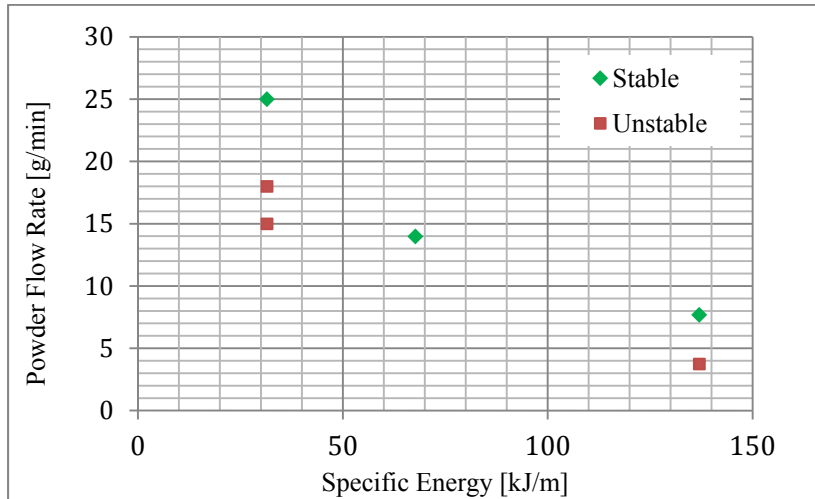

FIGURE 6: POWDER USE EFFICIENCY AND DEPOSITION STABILITY AS A FUNCTION OF SPECIFIC ENERGY

Stability in this study refers to how closely the actual deposition height corresponds to the z-step of the deposition head. If the deposition height is not high enough to accommodate the height of the programmed z-step, the position of the laser focus will begin to rise so that it is no longer buried in the substrate. This is a result of not enough powder being fed into the molten pool and is referred to as an under built condition. However, if too much powder is fed, the deposit will get too close to the laser and change the laser focus condition. This condition results in inconsistent layer deposits and is referred to as an over build condition. While the overbuild condition occurred to a small degree in test 2, for most of the trials, the under build regime dominated and was constantly requiring corrections to the supplied powder flow rate.

OBSERVATIONS

The effects of process variation across test settings are immediately apparent by examining of the metallographic cross-section. Shown in Figure 7(a) is the difference in deposit height between tests 1 and 2. Test 1 has the proper balance between powder feed, laser speed, and laser power; resulting in an individual layer height corresponding to the z-step of the deposition head. This balance results in a constant distance between the deposition head and the top of the deposit. The constant distance allows for a constant melt pool size, consistent width of deposited material, and a final component that accurately reflects the dimensions of computer model. Conversely in test 3 in Figure 7(a) the height is ~70% of the intended 1 inch. The initial settings for this deposit had a powder supply deficit relative to laser power and speed, which led to a layer height that was insufficient to match the z-step of the deposition head. The deficient layer height compounds over successive passes, yielding a component that is significantly under built.
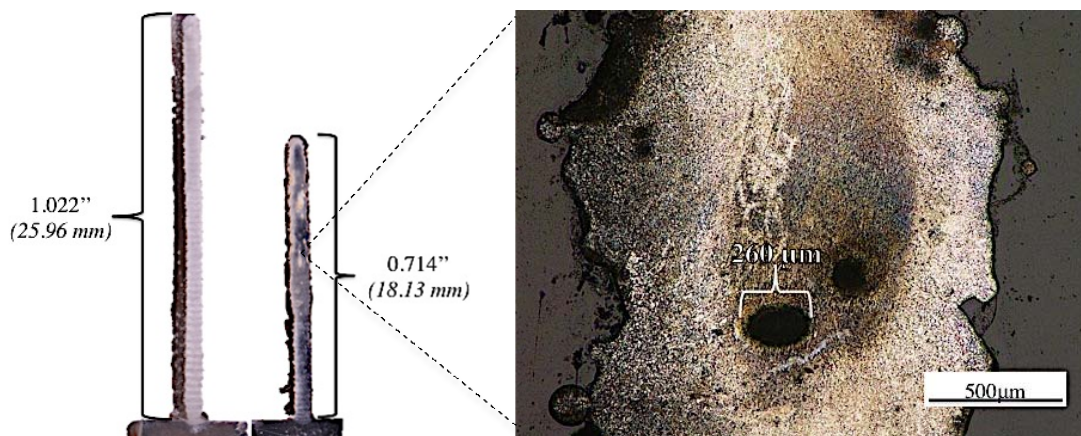

FIGURE 7: (LEFT) STEREOMICROGRAPH OF GEOMETRIC VARIATION BETWEEN TESTS 1 AND 3. (RIGHT) LARGE INTERNAL PORE DEFECT IN TEST 3.

Additionally in Figure 7(b) shows the macroscopic defects in the build that can form as a result of unstable deposition. The width of deposit in test 3 in nominally 1.4 mm, yet as a result of unstable deposition there is a 260 μm diameter closed pore in the center, with other porosity around it. These defects are not visible from the surface but would severely degrade performance if this was used as a structural component.

MELT POOL INSTABILITY

The recommended operating alignment for the LENS™ MR-7 is a focus that lies 0.305 mm (0.12 in.) above the deposit plane, as shown in Fig. 8. Note that if the substrate is pulled away from this point so that the spot size is increased, an overfeed situation occurs and the resulting deposit thickness is greater than what is intended. Conversely, a smaller spot size results in an underfeed situation and the deposit thickness is less than anticipated. Also note that these effects are magnified when multi-pass depositions are conducted.
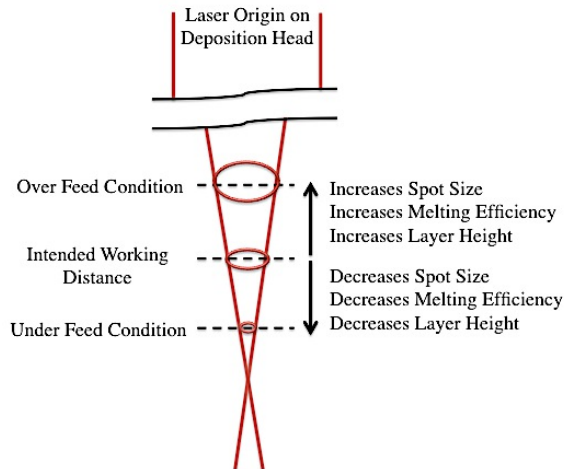
340

FIGURE 8: POSITIVE DIVERGENCE FEEDBACK

From the instabilities that were observed during deposition with a positive divergence feedback, it is clear that this is not the operational regime desired for such a dynamic process. The ideal set of process parameters result in a process that self-corrects so that it does not become unstable. One way to create a passive negative deposition feedback, is to move the deposition location to the far side of sharp laser focus. When the laser and deposition head are aligned to create this condition it will result in the schematic shown in Figure 9.
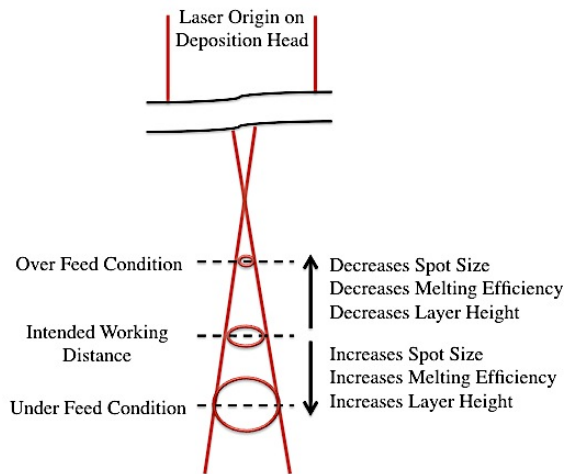

FIGURE 9: NEGATIVE DIVERGENCE FEEDBACK

When operating under positive divergence feedback, the deposition will self correct. For example, if the process is operating in an over feed condition; the spot size is decreased as is the melting efficiency and layer height. In contrast, if the process is operating in an under feed condition, the spot size is increased, as is the melting efficiency and layer height. Thus, multi-pass depositions will auto-correct over sequential layers.

341

CONCLUSIONS

Initial alignment and input parameters have a significant impact on the depositions produced by the LENS process. Deposition instability results from an inequality between laser speed, power, and powder feed, as well as a default positive divergence feedback. This instability leads to significant deviations between the intended height of a multi-pass deposit and the actual height. While inequalities persist regardless of feedback conditions, it was suggested that the divergence between intended and actual height can be eliminated by refocusing the laser so that deposition occurs on the opposite side of sharp laser focus (e.g. above the surface of the preceding deposit). Future research will explore the effects of operating on the far side of sharp focus, and further development of analytical models for stable deposition.

ACKNOWLEDGEMENTS

REFERENCES

[1] **Lewis, Gary K., et al.** *Directed Light Fabrication of Near-Net Shape Metal Components.* s.l. : Los Alamos National Laboratory: Materials Sceince and Technology Division, 1994.

[2] **Liou, Frank, *et al*.** *Applications of a Hybrid Manufacturing Process for Fabrication of Metallic Structures.* 2007. pp. 236-244.

[3] **Optomec Incorporated.** LENS^TM MR-7 User Manual

[4] **Heilbronner, Renee.** *How to Derive Size Distributions of Particles from Size Distrubitions of Sectional Areas.* Basel, Switzerland : Department of Earth Sciences, Basel University, 2002.

[5] **Xaio, Bin. *et al.*** *Partial Melting and Resolidification of Metal Powder in Selective Laser Sintering.* Journal of Thermophysics and Heat Transfer, 2006.